

# First Principles Study of Propene Polymerization in Ziegler–Natta Heterogeneous Catalysis

Mauro Boero,<sup>\*,†,‡</sup> Michele Parrinello,<sup>§</sup> Stephan Hüffer,<sup>||</sup> and Horst Weiss<sup>||</sup>

Contribution from the Max Planck Institut für Festkörperforschung, Heisenbergstrasse 1, D-70569 Stuttgart, Germany, Joint Research Center for Atom Technology (JRCAT), Angstrom Technology Partnership (ATP), 1-1-4 Higashi, Tsukuba, Ibaraki 305-0046, Japan, and BASF A.G., Polymer Physics and Solid State Physics Department and Polyolefines Department, D-67056 Ludwigshafen, Germany

Received March 22, 1999. Revised Manuscript Received November 15, 1999

**Abstract:** In this work we address the problem of isotacticity in a realistic heterogeneous Ziegler–Natta system by means of ab initio molecular dynamics. We focus on a previously identified 5-fold catalytic center, and we inspect its ability to select the appropriate olefin enantioface in the chain growth process. We study the first steps in the propene polymerization process and determine the energetics of the initial complexation phase for the different stereochemical orientations of the incoming propene. Then we analyze the subsequent insertions, which represent the crucial issue for the formation of a stereospecific polymer chain, and we find that the 5-fold catalytic center possesses a high degree of stereoselectivity. We examine the role of the agostic interaction, which can switch from  $\alpha$  to  $\beta$  and allow, even in the presence of a substrate, processes that can lead to chain termination.

## 1. Introduction

Ziegler–Natta (ZN) heterogeneous catalysis is nowadays the most important industrial process for the production of polyolefins, especially polypropylene. Over the past few decades, supported catalyst systems have had a great effect in improving the efficiency of polyolefins production, with enormous economic impact.

Although extensive studies on heterogeneous ZN catalysts have been made,<sup>1–12</sup> to unravel the basic steps in the catalytic

process, a deep understanding of the structure of the active centers and the role of the supporting surfaces is still needed. As a result, the development of industrial catalysts has been predominantly a matter of trial and error. On the theoretical front, the difficulty in modeling a heterogeneous system has so far limited ab initio investigations, which have more recently focused mostly on homogeneous catalysts.

One of the major obstacles is the need to include a realistic description of the substrate in the calculation. This need leads to very large systems and can be prohibitively expensive in standard quantum chemical approaches. Nevertheless, the substrate plays a crucial role both at the stage of the formation of the catalyst sites and in the polymerization process. In fact, phenomena that can occur in a homogeneous system, where large portions of empty space exist around the catalyst, can be blocked or hindered to a varying extent by the presence of a wide support. Furthermore the support can exert other forces (for instance coulomb forces) on the growing chain and interfere in many ways with the polymerization process. Thus, it is of fundamental importance to improve our understanding of this class of catalysts and to obtain the insight needed for a rational improvement of the industrial process.

Very recently we have made an important stride in this direction<sup>13</sup> by simulating the polymerization of ethylene via a

\* Author to whom correspondence should be addressed.

† JRCAT.

‡ On leave from the Max Planck Institut für Festkörperforschung.

§ Max Planck Institut für Festkörperforschung.

|| BASF A.G.

(1) (a) Corradini, P.; Busico, V.; Guerra, G. *Comp. Polym. Sci.* **1988**, *4*, 29–50. (b) Corradini, P.; Barone, V.; Fusco, R.; Guerra, G. *Eur. Polym. J.* **1979**, *15*, 133. (c) Busico, V.; Corradini, P.; De Martino, L.; Proto, A.; Albizzati, E. *Makromol. Chem.* **1986**, *187*, 1115. (d) Busico, V.; Cipullo, R.; Corradini, P.; De Biasio, R. *Macromol. Chem. Phys.* **1995**, *196*, 491. (e) Cavallo, L.; Guerra, G.; Corradini, P. *J. Am. Chem. Soc.* **1998**, *120*, 2428.

(2) Pino, P.; Mühlaupt, R. *Angew. Chem.* **1980**, *92*, 869, and references therein.

(3) Terano, M.; Kataoka, T.; Keii, T. *J. Polym. Sci., Part A: Polym.* **1990**, *28*, 2035.

(4) Soga, K.; Shiono, T.; Doi, Y. *Makromol. Chem.* **1988**, *189*, 1531.

(5) (a) Magni, E.; Somorjai, G. A. *Catal. Lett.* **1995**, *35*, 205. (b) Magni, E.; Somorjai, G. A. *Appl. Surf. Sci.* **1995**, *89*, 187. (c) Magni, E.; Somorjai, G. A. *Surf. Sci.* **1996**, *345*, 1.

(6) (a) Albizzati, E.; Giannini, U.; Morini, G.; Smith, C. A.; Ziegler, R. C.; *Ziegler Catalysts*; Fink, G.; Mühlaupt, R.; Brintzinger, H. H., Eds.; Springer-Verlag: Berlin, Heidelberg, 1995; p 413, and references therein. (b) Albizzati, E.; Giannini, U.; Balbontin, G.; Camurati, I.; Chadwick, J. C.; Dall'Occo, T.; Dubitsky, Y.; Galimberti, M.; Morini, G.; Maldotti, A. *J. Polym. Sci., Part A: Polym. Chem.* **1997**, *35*, 2645.

(7) (a) Xu, J. T.; Feng, L. X.; Yang, S. L. *Macromolecules* **1997**, *30*, 2539. (b) Xu, J. T.; Feng, L. X.; Yang, S. L.; Wu, Y. N.; Yang, Y. Q.; Kong, X. M. *Macromol. Rapid Comm.* **1996**, *17*, 645.

(8) (a) Kawamura-Kuribayashi, H.; Koga, N.; Morokuma, K. *J. Am. Chem. Soc.* **1992**, *114*, 2359. (b) Shiga, A.; Kawamura-Kuribayashi, H.; Sasaki, T. *J. Mol. Catal.* **1995**, *98*, 15. (c) Shiga, A. *J. Macromol. Sci., A* **1997**, *34*, 1867.

(9) Colbourn, E. A.; Cox, P. A.; Carruthers, B.; Jones, P. J. V. *J. Mater. Chem.* **1994**, *4*, 805.

(10) (a) Ferriera, M. L.; Juan, A.; Castellani, N. J.; Damiani, D. E. *J. Mol. Catal.* **1994**, *87*, 137. (b) Ferriera, M. L.; Castellani, N. J.; Damiani, D. E.; Juan, A. *J. Mol. Catal., A* **1997**, *122*, 25. (c) Ferriera, M. L.; Marta Branda, M.; Juan, A.; Damiani, D. E. *J. Mol. Catal., A* **1997**, *122*, 51.

(11) Mosley, D. H.; Denil, C.; Champagne, B.; André J–M. *J. Mol. Catal., A* **1997**, *119*, 235.

(12) Jensen, V. R.; Børve, K. J.; Ystenes, M. *J. Am. Chem. Soc.* **1995**, *117*, 4109.

(13) (a) Boero, M.; Parrinello, M.; Terakura, K. *J. Am. Chem. Soc.* **1998**, *120*, 2746. (b) Boero, M.; Parrinello, M.; Terakura, K. *Proc. of ISSI PDSC-98*, Elsevier: Tokyo; 19–21 November 1998.

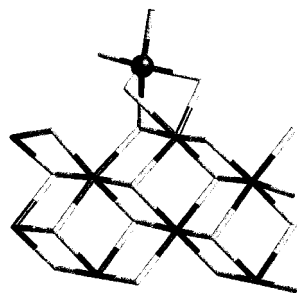


**Figure 1.** The 5-fold Ti site on the (110) surface of  $\text{MgCl}_2$ . The chirality of this configuration can be seen from the figure. For the sake of clarity, here and in the following figures, only the structure around the active site is shown, and the actual size of the supercell is reported in the text. The Ti is evidenced with a ball, the crossing points of the gray sticks indicate the position of the Cl atoms, and the crossing points of the black sticks indicate the Mg atoms.

realistic heterogeneous ZN system using Car–Parrinello<sup>14</sup> molecular dynamics (CPMD). In this study, we found that a highly probable catalytic species is a 5-fold coordinated Ti site,<sup>15</sup> reported in Figure 1, obtained by depositing a  $\text{TiCl}_4$  molecule on the (110) surface of  $\text{MgCl}_2$ , which is industry's support for high-yield catalysts. However, this study could not address one of the most successful features of ZN catalysis, namely its stereoselectivity, because this issue is irrelevant for ethylene. In general terms, stereoselectivity has to be linked to the chirality of the ZN catalytic center.<sup>16,17</sup> However, no detailed quantitative description of the stereoselection mechanism has so far been given, and our calculations represent the first detailed fully ab initio study of polymer stereoregularity in an industrial process.

We show in the following that the very same 5-fold coordinated Ti site of our previous study<sup>13</sup> can also catalyze the polymerization of polypropylene and has the desired stereoselective properties. The substrate plays a crucial role in promoting stereoregularity. We also assess the role of agostic interaction both in determining the transition state energetics and in allowing for the possibility of chain termination processes. A detailed study of the changes in the electronic structures during the reaction will be presented by making use of a recently developed Wannier centers methodology.<sup>18</sup>

## 2. Computational Method

We adopted a Becke–Lee–Yang–Parr<sup>19</sup> (BLYP) gradient-corrected density functional approach<sup>20</sup> and performed CPMD simulations<sup>21</sup> on a system containing 24 formula units of the substrate of  $\text{MgCl}_2$  and

(14) Car, R.; Parrinello, M. *Phys. Rev. Lett.* **1985**, *55*, 2471.

(15) Both static relaxations of the nonactivated 5-fold site, performed after the deposition, and finite temperature molecular dynamics simulations during the polymerization reaction have shown that this configuration does not relax/convert to a different geometry or gives rise to changes in the coordination of the Ti site. Thus, under the reported simulations conditions, the present catalyst configuration is a stable structure.

(16) (a) Busico, V.; Corradini, P.; De Martino, L.; Proto, A.; Savino, V. *Makromol. Chem.* **1985**, *186*, 1279. (b) Zambelli, A.; Locatelli, P.; Sacchi, M. C.; Rigamonti, E. *Macromolecules* **1980**, *13*, 798.

(17) Veghini, D.; Henling, L. M.; Burkhardt, T. J.; Bercaw, J. E. *J. Am. Chem. Soc.* **1999**, *121*, 564.

(18) (a) Wannier, G. H. *Phys. Rev.* **1937**, *52*, 191. (b) Marzari, N.; Vanderbilt, D. *Phys. Rev. B* **1997**, *56*, 12847. (c) Silvestrelli, P. *Phys. Rev. B* **1998**, *59*, 9703.

(19) (a) Becke, A. D. *Phys. Rev. A: At., Mol., Opt. Phys.* **1988**, *38*, 3098. (b) Lee, C.; Yang, W.; Parr, R. G. *Phys. Rev. B: Condens. Matter* **1988**, *37*, 785.

(20) We stress the fact that a simple LDA approach turned out to be insufficient, because it overestimates binding energies and largely underestimates activation barriers as reported in ref 13. The importance of proper inclusion of correlations in first principles calculations has already been pointed out in previous works.<sup>22</sup> For a general review on the performances of density functional methods see, for example, ref 23.

one active Ti(IV) center. The semi-infinite surface (110) is approximated by a slab, which is 6 layers thick. On the lower part of the slab, the atoms are kept fixed, while the catalyst and the growing polymer chain are placed on the other side. We have explicitly taken into account so many layers because surface relaxation propagates rather deeply, as discussed previously.<sup>13</sup> Because we use plane waves as basis set, we have to impose periodic conditions, which implies that the supercell is repeated not only in the plane of the slab but also in the direction perpendicular to it. We have used a monoclinic supercell of size  $12.729 \times 11.782 \times 27.512 \text{ \AA}^3$  and an angle of  $72^\circ$ . The use of this supercell allows us to ignore the interaction between each cell and its periodic images and leaves enough space between the slabs to accommodate the catalyst and the growing polymer. The periodically repeated images of the Ti active center in the  $x$  and  $y$  directions are separated from each other by  $12.729 \text{ \AA}$ .

The norm-conserving pseudopotentials of Trouiller and Martins,<sup>24</sup> including nonlinear core corrections<sup>25</sup> for Mg and Ti, accounted for the valence–core interactions. Valence electrons are treated explicitly in a plane wave basis set with an energy cutoff of 40 Ry, and the Brillouin zone of the supercell is sampled only at the  $\Gamma$  point.

For constrained dynamics,<sup>26,27</sup> the integration time step was set to 5 au, the equilibration time was 1.5 ps (as adopted for the case of ethylene), and the holonomic constraint was linearly added to the CP Lagrangean via Lagrange multiplier as described in ref 13.

Further computational details will be given in the following sections whenever they are necessary to support the discussion.

## 3. Results and Discussion

In the following, we shall consider the formal oxidation state of the catalyst to be Ti(IV). Although other possibilities are not excluded,<sup>28</sup> we based our choice on the recent extended X-ray absorption fine structure (EXAFS) experiments<sup>29</sup> and on indications from industry,<sup>30,31</sup> which identified Ti(IV) as the dominant catalytic species.

The high reactivity of the Ti 5-fold center has already been discussed.<sup>13</sup> For ethylene, the relevant energetics was found to be such that ethylene is likely to be one of the most important reaction centers. We shall show here that the same center plays

(21) We have used the code CPMD, version 3.0f, developed by J. Hutter, P. Ballone, M. Bernasconi, P. Focher, E. Fois, S. Goedecker, D. Marx, M. Parrinello, and M. Tuckerman, at MPI für Festkörperforschung and IBM Zurich Research Laboratory (1990–1997). The Wannier Functions calculation in the implementation of P. L. Silvestrelli, S. Rauegi, and M. Boero was adopted. The code was ported on VPP-Fujitsu by M. Boero.

(22) (a) Weiss, H.; Ehrig, M.; Ahlrichs, R. *J. Am. Chem. Soc.* **1994**, *116*, 4919. (b) Fan, L.; Harrison, D.; Woo, T. K.; Ziegler, T. *Organometallics* **1995**, *14*, 2018. (c) Woo, T. K.; Fan, L.; Ziegler, T. *Organometallics* **1994**, *13*, 2252.

(23) (a) Johnson, B. G.; Gill, P. M. W.; Pople, J. A. *J. Chem. Phys.* **1993**, *98*, 5612. (b) Pis-Diez, R. *Chem. Phys. Lett.* **1998**, *287*, 542.

(24) Trouiller, N.; Martins, J. L. *Phys. Rev. B: Condens. Matter* **1991**, *43*, 1993.

(25) Louie, S. G.; Froyen, S.; Cohen, M. L. *Phys. Rev. B: Condens. Matter* **1982**, *26*, 1738.

(26) (a) Ciccotti, G.; Ferrario, M.; Hynes, J. T.; Kapral, R. *Chem. Phys.* **1989**, *129*, 241. (b) Carter, E. A.; Ciccotti, G.; Hynes, J. T.; Kapral, R. *Chem. Phys. Lett.* **1989**, *156*, 472. (c) Paci, E.; Ciccotti, G.; Ferrario, M.; Kapral, R. *Chem. Phys. Lett.* **1991**, *176*, 581. (d) Ciccotti, G.; Ferrario, M. *Monte Carlo and Molecular Dynamics of Condensed Matter Systems*, Proc. of Euroconf. on Computer Simulation in Condensed Matter Physics and Chemistry; Binder, K.; Ciccotti, G., Eds.; SIF: Como, 1995.

(27) (a) Mülders, T.; Krüger, P.; Swegat, W.; Schlitter, J. *J. Chem. Phys.* **1998**, *104*, 4869. (b) den Otter, W. K.; Briels, W. J. *J. Chem. Phys.* **1998**, *109*, 4139. (c) Sprik, M.; Ciccotti, G. *J. Chem. Phys.* **1998**, *109*, 7737.

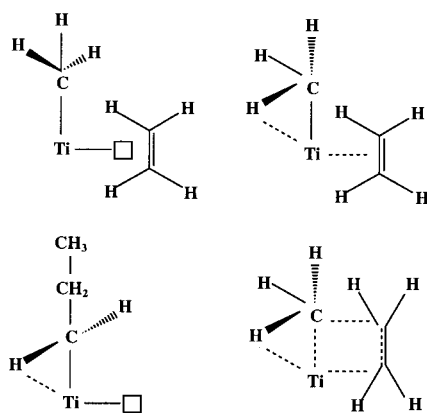
(28) (a) Magni, E.; Somorjai, G. E. *J. Phys. Chem. B* **1998**, *102*, 8788. (b) Korányi, T. I.; Magni, E.; Somorjai, G. E. *Top. Catal.* **1999**, *7*, 179.

(29) Jones, P. J. V.; Oldman, R. J. *Transition Metals and Organometallics as Catalysts for Olefin Polymerization*; Kaminsky, W.; Sinn, H., Eds.; Springer-Verlag: Berlin, 1988; p 223.

(30) Hüffer, S., *private communication*.

(31) We do not claim that the Ti oxidation state is always IV in any Ziegler–Natta heterogeneous system. Nevertheless we have evidence from industry and experiments that Ti(IV) is an active species in the real polymerization process.

## Scheme 1



an important role for propene and has strong stereoselective properties. However, before moving to propene, it is useful to recall briefly the main findings on ethylene in view of the analogies and differences that will be discussed in the following paragraphs. In the case of ethylene, the first step in the polymerization process was the complexation of the monomer with the activated 5-fold site, leading to the so-called  $\pi$ -complex. This process was barrierless and led to an energy gain. From the  $\pi$ -complex, the reaction proceeds via a transition state, to which is associated a barrier of 6.7 kcal/mol. Here, as in the following, we will measure the transition barriers relative to that of the  $\pi$ -complex. The reaction pathway is shown in Scheme 1 which, as proposed by the Cosse–Arlman<sup>32</sup> mechanism reviewed by Brookhart and Green,<sup>33</sup> is  $\alpha$ -agostic assisted via a tilt of the methyl group.

The final product is characterized by an energy gain of  $-23.3$  kcal/mol. Our simulation also evidenced a very interesting and unexpected feature of the polymerization in the successive ethylene insertions; namely, further ethylene additions cause the chain to drop along the substrate, leaving one side of the active center unshielded and available for subsequent complexation and insertion processes. This feature rules out the flip–flop mechanism that has usually been assumed to hold for homogeneous catalysis and makes the nonhomogeneous catalytic process rather different. In the subsequent insertions, the activation energy, as measured from the  $\pi$ -complex, was 6.1 kcal/mol and the process turned out to be  $\beta$ -agostic assisted due to the geometrical arrangement of the polymer chain after its spontaneous displacement along the support. From the second insertion onward, the olefin addition process followed this path, making the first insertion somewhat atypical and underscoring the need to simulate the process in all its complexity. Further details can be found in the already quoted reference.<sup>13</sup>

**3.1. Propene Insertion Reaction.** We now proceed to study the first propene insertion on the 5-fold activated site, where one of the Cl has already been replaced by the chain terminator (in this case, a  $\text{CH}_3$  methyl group). The major changes relative to the ethylene case come from the extra steric interaction due to the  $\text{CH}_3$  residue of the propene molecules, which hinders the approach of the propene molecule to the catalytic center. One first major effect is the reduction of the complexation energy, which is only 3.6 kcal/mol as compared with the 24.0 kcal/mol in the case of ethylene. This difference is due to the fact that here the Ti–alkene distance is much larger, resulting

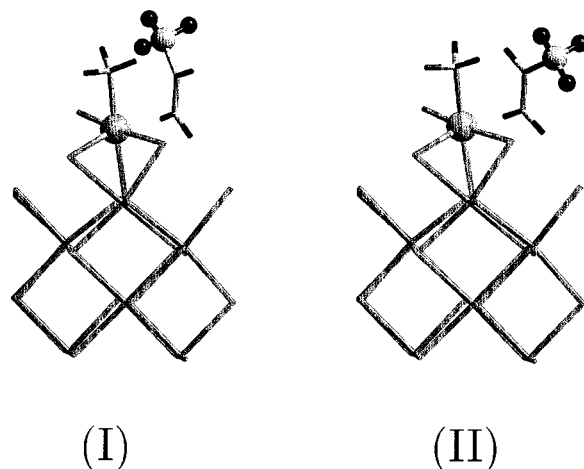


**Figure 2.** The two possible  $\pi$ -complex enantiofaces (I) and (II) relevant to the first propene insertion in the 5-fold-activated Ti(IV) site. In this figure as well as in the following ones, the methyl group of the propene molecule(s) and the metal catalyst are evidenced with balls.

**Table 1.** Energetics for the Insertion of the First Propene in the 5-Fold Active Site<sup>a</sup>

enantioface	$\pi$ -complex	transition state	product
(I)	0.0	10.8	$-16.7$
(II)	1.7	13.9	$-12.6$
(I) <sup>b</sup>	0.0	10.5	$-17.8$
experiment <sup>c</sup>		9.5–12.0	

<sup>a</sup> Values in kcal/mol. <sup>b</sup> Second insertion. <sup>c</sup> Reference 42.

in a lower complexation energy.<sup>34</sup> The steric interaction is so large that the  $\pi$ -complex is bound only if the propene is either oriented as in (I) (Figure 2(I)) or as in (II) (Figure 2(II)). In these two orientations, the formation of the complex is still barrierless. Any attempt at stabilizing the other two orientations, in which the  $\text{CH}_3$  group points to the support, failed and the propene spontaneously flew away. The two enantiofaces (I) and (II) have similar behavior and follow essentially the same reaction pathway as ethylene, differing only slightly in the energetics and in some geometrical details. Enantioface (I) (Figure 2(I)) gives the lowest complexation energy (3.6 kcal/mol), has a barrier for the first insertion of 10.8 kcal/mol, which is much larger than that of ethylene (6.7 kcal/mol), and is  $\alpha$ -agostic assisted. Enantioface (II) has a complexation energy that is lower by 1.7 kcal/mol because of the additional steric interaction, which leads to an extra rotation of the methyl group of  $14^\circ$  around the Ti–C axis. The activation energy is also slightly larger for enantioface (II) for very similar reasons (see Table 1). The insertion is also in this case  $\alpha$ -agostic assisted. In Figure 3, the similarity between the final state in (I) and (II) can also be seen. This similarity is even more accentuated when we proceed to a second isotactic insertion, as shown in Figure 4. As in the case of ethylene the chain is displaced along the substrate, leading to two mirror situations corresponding to a *si*-coordinated monomer as in Figure 4a and its symmetric case. In either structure the chain arranges itself so as to minimize the interaction of the two bulky  $\text{CH}_3$  groups with the support. In both cases it is the smaller  $\text{H}_\beta$  unit that points toward the  $\text{MgCl}_2$  surface.

In case of enantioface (II), one could in principle argue that the olefin approach to the active site could occur in a *re*

(32) (a) Cossee, P. *J. Catal.* **1964**, *3*, 80. (b) Arlman, E. *J. Catal.* **1964**, *3*, 89. (c) Arlman, E.; Cossee, P. *J. Catal.* **1964**, *3*, 99.

(33) Brookhart, M.; Green, M. L. H. *J. Organomet. Chem.* **1983**, *250*, 395.

(34) In the case reported in Figure 2(a), we found Ti–C<sub>1</sub> = 2.993 Å and Ti–C<sub>2</sub> = 2.826 Å, which can be compared with the analogous results for ethylene of Ti–C<sub>1</sub> = 2.876 Å and Ti–C<sub>2</sub> = 2.804 Å (where C<sub>1</sub> and C<sub>2</sub> are the carbons bound by the double bond in the propene molecule).

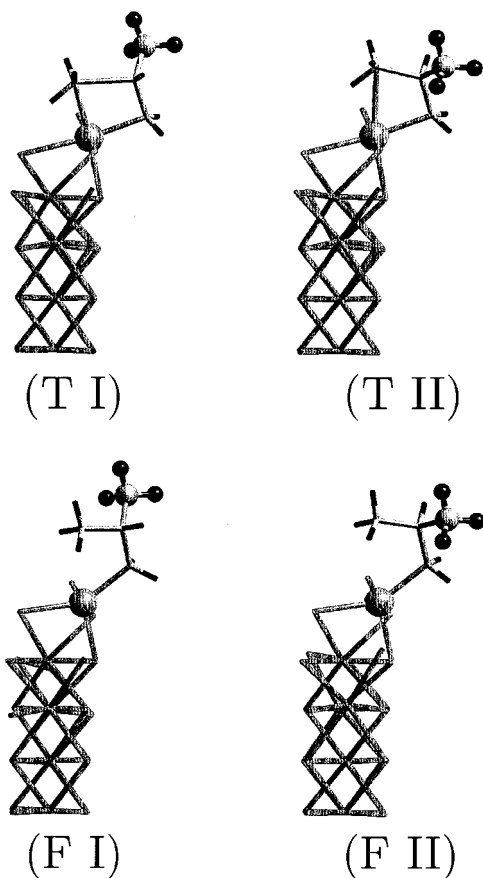


**Figure 3.** The transition states (T I) and (T II), relevant to enantiofaces (I) and (II) and the corresponding final products (F I) and (F II), respectively (see text for details).

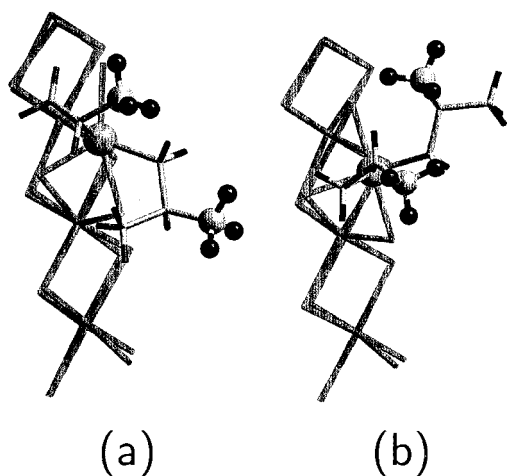


**Figure 4.** Reorientation of the polymer chain as a response to a new propene complexation. The chain geometry (a) results from enantioface (I) in the *si* orientation and the chain geometry (b) from a possible *re* insertion from enantioface (II). In case (a) the equilibrium Ti–C $_{\alpha}$  distance is 2.164 Å while in case (b) the distance elongates to 2.239 Å.

configuration as in Figure 4b, but in this case the relative orientations of the monomer and the chain are such that the steric repulsion increases and locates the complex at 3.2 kcal/mol higher in energy than in the *si* case. This point will be further discussed in the paragraph relevant to the second insertion.

From these observations it is clear that the stereoselectivity does not depend on the chosen monomer enantioface for the

first insertion: all the conclusions that can be drawn by studying one of the two chain conformations can be repeated with only minor changes for the other. For this reason, and to limit the computational effort, we shall restrict our analysis to the case of enantioface (I), which is also slightly favored in energetics. The behavior of enantioface (II) will be very similar.

**3.2. Evolution of the Electronic States during the Propene Insertion.** To follow the evolution of the electronic states during the reaction we shall use the maximally localized wave functions introduced in ref 18, which are the extension to a periodic system of the well-known Boys<sup>35</sup> localized orbitals. However, because the full information contained in the Wannier function is difficult to represent, we will contract this information drastically and monitor only the center of mass of the Wannier functions or Wannier Functions Centers (WFCs), defined in ref 18 as  $x_i = -(L/2\pi) / m \ln \langle w_i | \exp(-ix \cdot 2\pi/L) | w_i \rangle$  and their spacial dispersion  $\sigma_i = \langle x^2 \rangle_i - \langle x \rangle_i^2$ , where  $L$  is the supercell dimension in the  $x$  directions (analogous definitions hold along  $y$  and  $z$ ),  $w_i$  is the  $i$ th Wannier function, and  $\langle \dots \rangle_i$  indicates the expectation value with respect to the  $i$ th Wannier state. This method has been shown to provide a vivid picture of the chemistry in many systems,<sup>36</sup> and the same holds here.<sup>37</sup>

We use the method of lagrangean constraint to study the reaction process. As reaction coordinate we have chosen  $\xi = |C_{\alpha} - C_{\text{prop}}|$ , which is the distance between the C $_{\alpha}$ -atom of the chain (methyl group bound to Ti) and the C atom of the incoming propene carrying the CH $_3$  group (C $_{\text{prop}}$ ). This distance, of course, is the one that leads to the formation of the new bond between the incoming olefin and the growing polymer chain.

In the case of an isolated propene, the double carbon bond reflects itself in two Wannier centers, W $_{p1}$  and W $_{p2}$ , symmetrically located at 0.346 Å from the middle of the C=C axis, as in Figure 5(a). When the  $\pi$ -complex is formed, W $_{p1}$  and W $_{p2}$  are pulled toward the catalyst (see Figure 5(b)). At the transition state (Figure 5(c)), W $_{p1}$  binds the carbon atom that in the chain will become C $_{\alpha}$  to the titanium, while W $_{p2}$  and W $_{Ti}$  are ready to form the single carbon bonds of the polymeric chain reported in Figure 5(d). The displacement of W $_a$  is also worthy of note because it clearly reflects the formation of the agostic interaction that is also apparent from the tilt of the chain-terminating CH $_3$  group. Note that at the transition state, W $_a$  displaces by as much as 0.149 Å from the C–H axis and points toward the Ti.

We made this method more quantitative by monitoring the geometrical evolution of these WFCs as the reaction proceeds. The evolution of the WFCs is given in terms of their distances from the original bond to which they belong in the complex configuration. In particular, in Figure 6, we refer to W $_{p1}$  and W $_{p2}$  as the distances of these centers from the carbon double

(35) Boys, S. F. *Quantum Theory of Atoms, Molecules and the Solid State*; Löwdin, P. O., Ed.; Academic: New York, 1966; p 253.

(36) (a) Silvestrelli, P. L.; Marzari, N.; Vanderbilt, D.; Parrinello, M. *Solid State Comm.* **1998**, *107*, 7. (b) Silvestrelli, P. L.; Parrinello, M. *Phys. Rev. Lett.* **1999**, *82*, 3308. (c) Boero, M.; Parrinello, M.; Terakura, K. *Maximally Localized Wannier Functions: An Application to Chemical Reactions*. In *1998 JRCAT International Symposium on Atom Technology Proc.*, Komaba Eminence: Tokyo, 1998; p 349. (d) Billas, I. M. L.; Massobrio, C.; Boero, M.; Parrinello, M.; Branz, W.; Tast, F.; Malinowski, N.; Heinebrodt, M.; Martin, T. P. *J. Chem. Phys.*, in press.

(37) All the representations of the wave functions related by a unitary transformation are of course equivalent and could suit the scope of monitoring the changes in the electronic structure. However, the one that we chose gives us an unbiased way to split up the global information contained in the electronic density  $\rho(\mathbf{x})$  without making system-dependent assumptions or an ad hoc hypothesis. From the computational point of view, contracting the orbital information to only four numbers (i.e., the WFC position  $(x_i, y_i, z_i)$  and its dispersion  $\sigma_i$  instead of the whole array  $|\psi_i(x, y, z)|^2$ ) allows us to save a lot of storing time and disk space while following the time evolution of the process.

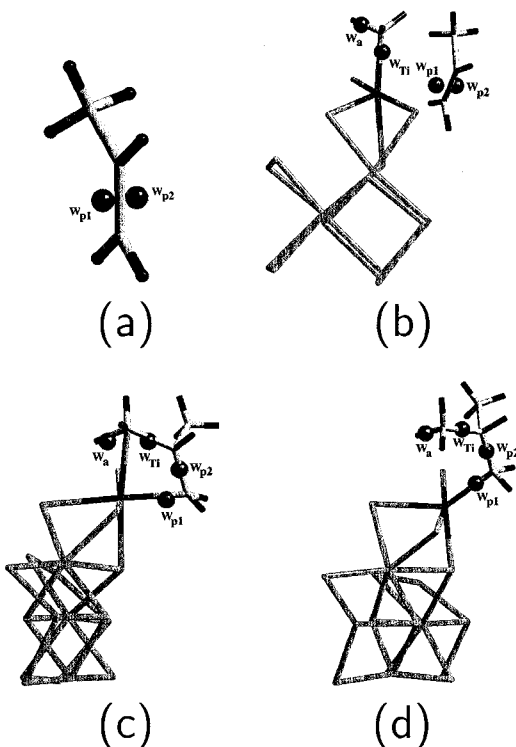


**Figure 5.** Main WFCs relevant to (a) the isolated propene molecule; (b) the  $\pi$ -complex; (c) the transition state; and (d) the final product. In this figure, the balls represent the WFCs and the atomic structure is indicated by sticks only for the sake of clarity. The WFCs relevant to the process are labeled as  $W_{p1}$ ,  $W_{p2}$  (the WFCs relevant to the propene carbon double bond),  $W_{Ti}$  (the WFC of the metal–carbon bond), and  $W_a$  (the WFC involved in the agostic interaction). Further details are given in the text.

bond of the propene;  $W_{Ti}$  is the distance of the WFC located along the Ti–CH<sub>3</sub> bond from the metal–carbon bond itself and  $W_a$  is the off-axis displacement of the C–H center on the methyl group as a consequence of the  $\alpha$ -agostic interaction. We noticed that the WFC  $W_{Ti}$ , which in the  $\pi$ -complex was located along the Ti–CH<sub>3</sub> bond, displaces in the vicinity of the new bond that forms between the incoming propene and the C atom of the methyl group as the reaction proceeds. At the same time, the WFC indicated as  $W_a$ , which in Figure 5(b) was located on the C–H axis with C being the carbon atom of the methyl group, displaces off-axis up to 0.149 Å toward the Ti (transition state), and its distance from the catalytic center reduces to 1.871 Å from 2.388 Å ( $\pi$ -complex value) along the plot.

The larger changes in the positions of the WFCs occur starting from a value of the reaction coordinate of  $\sim 2.313$  Å (see Figure 6). The dispersions associated with the WFCs  $W_{p1}$  and  $W_{Ti}$  increase during the reaction as a consequence of the charge transfer involved in the construction of the new bonds between the propene and the catalyst ( $W_{p1}$ ) and the propene and the methyl group ( $W_{Ti}$ ) accompanied by the cleavage of the *old* Ti–CH<sub>3</sub> bond. Analogously, the dispersion associated with  $W_a$  increases because of the agostic interaction involving the metal and the H of the CH<sub>3</sub> group. The WFC  $W_{p2}$ , on the other hand, shows a slight reduction in its dispersion because the center is collapsing on the C–C bond during the reaction; that is, the bond is transforming from a double to a single bond, for which the WFC is more localized and coaxial. This analysis provides a comprehensive picture and, in particular, a very useful tool to identify the agostic interaction in terms of the electronic distribution, a detail that can escape other kinds of analysis like total charge distribution or electron localization function (ELF).

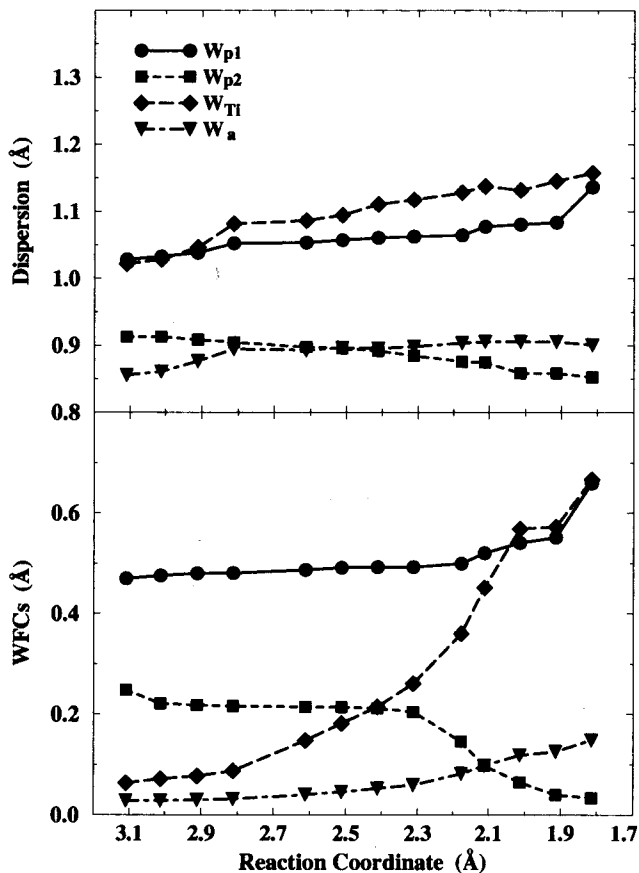


**Figure 6.** Evolution of the main WFCs and their related dispersions along the reaction coordinate as described in the text. Full circles refer to the center  $W_{p1}$ , squares to the center  $W_{p2}$ , diamonds to the center  $W_{Ti}$ , and triangles to the center  $W_a$  according to the labeling of Figure 5. The lines are intended only as a guide to the eye.

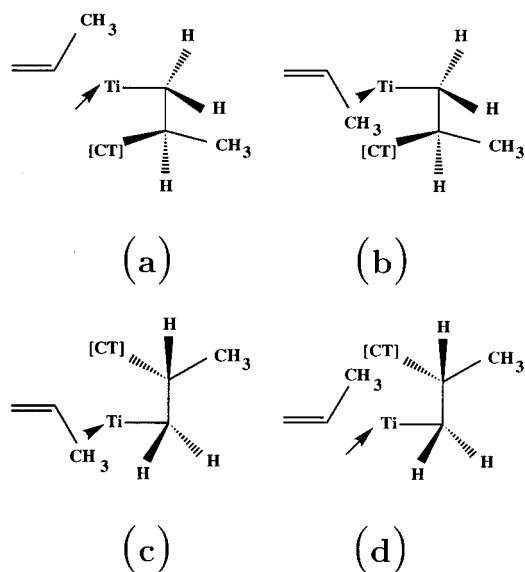
Of course, from the transition state on, because new bonds are formed and old bonds destroyed, it makes no sense to look at the distance of each WFC from its original bond. For this reason, our analysis jumps directly to the final product. The product is reported in Figure 5(d) which shows all the WFCs located on the proper bond axes, as is expected in ordinary single bonds.

**3.3. Chain Propagation.** The decisive step for the stereoselectivity is the next one. As observed, the approach of a second propene to the active center causes a reorientation of the polymer chain along the substrate in a way similar to the case of ethylene. The  $\gamma$ -agostic product, resulting from the chain initiation described in the previous paragraph, becomes an  $\alpha$ -agostic structure. Of course, because of the larger steric encumbrance of the CH<sub>3</sub> groups, the chain displacement is limited by the requirement that these groups have to stay far from the substrate.

Given the geometry of the chain at the end of the first insertion, a new propene molecule can approach the catalytic center in different ways. The key configurations relevant to the stereoselectivity problem are sketched in Scheme 2, where [CT] indicates the chain terminator and the arrow indicates the direction of one of the Cl atoms around the catalyst, which is useful for the following discussion.

In Figure 7 the corresponding geometries used in the calculations are shown from a top view. Figure 7(a) shows a *si*-oriented structure, whereas Figures 7(b) and (c) both refer to possible *re*-configurations. The  $\pi$ -complexes leading to 2,1 insertions would instead correspond to structures leading to regio errors. The regioselectivity of the 5-fold site will be considered

## Scheme 2



in detail in a forthcoming publication.<sup>38</sup> However, we anticipate here that the activation barriers associated with 2,1 insertions are, in agreement with previous experiments,<sup>39,40</sup> much higher than the regular 1,2 insertions and that the complexes are generally destabilized by steric interactions with the Cl atoms around the catalyst. At this stage, however, these conformations do not need to be considered for the issue of the stereoselectivity of the 5-fold site.

In Scheme 2, the chains sketched in (a) and (b) are the configurations as obtained after the first propene insertion in our simulations with the incoming propene in the *trans* and *cis* orientations, respectively. However, the chain might perform a rotation of 180° around the Ti–C<sub>α</sub> bond.<sup>41</sup> This rotation would lead to a structure with the growing polymer chain pointing roughly in the same direction of a Cl atom in the neighborhood of the active center (see Scheme 2(c) and (d)). These chain orientations differ in the propene methyl group, which is either in a *trans* (Figure 7(c) and Scheme 2(c)) or a *cis* (Scheme 2(d)) conformation relative to the C<sub>α</sub>–C<sub>β</sub> bond. We observe that the structures 7(a) and 7(c) (i.e., the *trans* conformers) would lead to asymmetric configurations (i.e., to stereoregions) if they had the same probability. We can relate these probabilities to the corresponding activation barriers. The same argument holds for structures (b) and (d) of Scheme 2 (i.e., the *cis* conformations). A site is considered to be stereoselective if one of these four conformations is energetically favored by an activation barrier sufficiently lower than its competitors. This is simply assessed on the grounds of Boltzmann statistics: given a RT value of ~0.8 kcal/mol, a difference of ~4 kcal/mol for the lowest activation barrier and its best competitor would lead to a stereoselectivity of >99%.

In the present case, only when a molecule is oriented as in (a) and (c) can a  $\pi$ -complex be formed in a barrierless way. In the other two cases, steric hindrances of the methyl group of the incoming propene and the growing polymer chain prevent

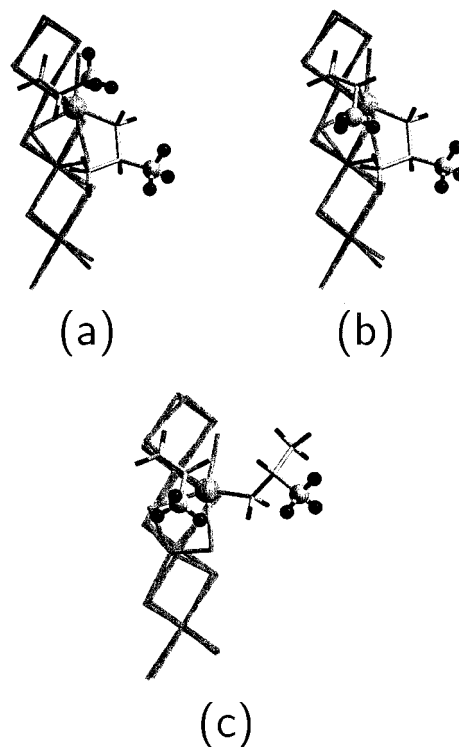


**Figure 7.** Possible  $\pi$ -complexes relevant to the polymer chain as obtained after the first insertion with enantioface (I). Only the *si* geometry (a) gives rise to a stable  $\pi$ -complex. The structures are labeled as in Scheme 2, (a), (b), and (c). The nearby MgCl<sub>2</sub> layers are not shown for the sake of clarity. The growing polymer chain occupies the open sector of the chiral coordination sphere; the propene has the enantiofacial orientation which leaves the olefin substituent *trans* to the polymer chain with respect to the C–C bond ((a), *si*-coordinated olefin). A *cis* orientation of olefin substituent and polymer chain is unfavored ((b), *re*-oriented olefin) because the chain points into a sector of the chiral coordination sphere which is occupied by a Cl atom. Structure (c) (*re*-oriented olefin) is also disfavored because the chain points into the sector of the chiral coordination sphere that is occupied by a Cl atom.

the formation of a stable complex and, for similar reasons, give rise to transition states that are energetically much higher (~7.6 kcal/mol). The activation barrier for the insertion reaction in the case of (c) is ~7.1 kcal/mol higher in energy, due to the strong repulsive interaction of the growing polymer chain and the nearest chlorines of the substrate. In fact, because in this case the polymer chain is rotated of 180° with respect to Figure 7(a) and (b), at least one of the CH<sub>3</sub> groups (or the [CT]) along the chain turns out to be closer to the substrate, thus interacting sterically with the Cl atoms at the surface of either the layer shown in Figure 7 or the nearby layer (not shown). This phenomenon is reflected in the unusually long Ti–C<sub>α</sub> bond, which is elongated from 2.100 to 2.213 Å in the case of the geometry shown in Figure 7(c). The conclusion that can be drawn from this finding is that, in this case, the substrate plays the role of the more bulky ligand in metallocene catalysis.<sup>42</sup> Here, as first proposed by Corradini's group<sup>1</sup> and by many other researchers, we have a so-called *indirect tacticity control*. The reaction mechanism resulting from the present simulations is that the growing polymer chain is oriented toward the regions with the lowest repulsive interactions with the ligands, whereas the propene is oriented in such a way that it minimizes the

(38) Boero, M.; Parrinello, M.; Weiss, H.; Hüffer S., manuscript in preparation.

(39) Kissin, Y. V. *Isospecific Polymerization of Olefins*; Springer-Verlag: New York, 1985.

(40) Allen, G. B. *Comprehensive Polymer Science*; Pergamon: Oxford, 1989.

(41) The standard notation is adopted, where  $\alpha$ ,  $\beta$ , etc. refer to the first, second, etc. carbon along the chain, the first C being the one bound directly to the metal.

(42) (a) Brintzinger, H. H.; Fischer, D.; Mülhaupt, R.; Rieger, B.; Waymouth, R. M. *Angew. Chem., Int. Ed.* **1995**, *34*, 1143, and references therein. (b) Corradini, P.; Guerra, G.; Vacatello, M.; Villani, V. *Gazz. Chim. Ital.* **1988**, *118*, 173.

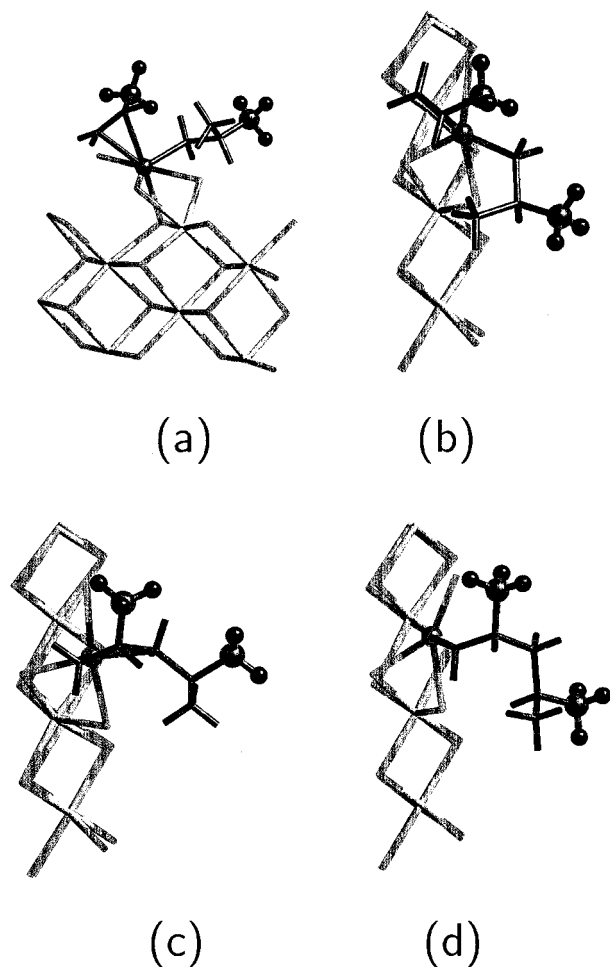


**Figure 8.** Main phases of the insertion of a second propene in the polymer chain: (a)  $\pi$ -complex (side view); (b)  $\pi$ -complex (top view); (c) transition state; and (d) final product.

repulsions with the chain; that is, the propene methyl group prefers a trans conformation with respect to the  $C_\alpha$ – $C_\beta$  bond. Thus, there is a perfect analogy with metallocene catalysis. In our case, we find the chain directed into the *free* space region as in Figure 7(a) and the role of the ligand is played by the substrate. The fact that this structure is  $\sim 7$  kcal/mol more stable than any other conformation reflects the strong stereoselectivity of the proposed active site.

Thus, the orientation in Figure 7(a) turns out to be that which leads to stereoselectivity; that is, the propene inserts itself into the  $\text{CH}_3$  group in the same position as the previous one. Figure 8 illustrates the main phases of this second propene insertion. This insertion takes place in a way similar to the first one, with an energy barrier of 10.5 kcal/mol (see Table 1), and it is  $\alpha$ -agostic assisted. This situation is different from the case of ethylene, where insertions from the second onward turned out to be  $\beta$ -agostic assisted. We stress again that this is the lowest barrier among all the other possible transition states relevant to other orientations of the olefin and the growing chain.<sup>43</sup> In summary, the orientation in Figure 7(a) turns out to be favored on two accounts: on one hand this orientation leads to a bound  $\pi$ -complex that enhances the probability of attempting a jump over the transition barrier, and on the other hand, the transition barrier is much lower.

From these observations, it is clear that this resulting stereoselectivity is a consequence of the local geometry of the active site carrying the growing chain, as experimentally proved for these catalytic systems, and is not a chain-end control effect,

as could be erroneously inferred by carelessly looking at the second insertion geometries.

Activation barriers of 10.5 kcal/mol, obtained in the successive insertions, are very close to the activation barriers of the first insertion and are in agreement with the reported theoretical estimates<sup>1,8</sup> and with experimental findings that point at a larger transition barrier for propene (9.5–12.0 kcal/mol)<sup>44</sup> than for ethylene. The reaction process leads to a gain in energy of 16.7 kcal/mol, which is lower than that of ethylene (23.3 kcal/mol). This difference is mainly due to a reduced freedom in the polymer chain reorientation that occurs, keeping the methyl groups as far as possible from the substrate for steric reasons.

**3.4. Switching from  $\alpha$ - to  $\beta$ -Agostic Interaction.** Like the first one, subsequent insertions are agostic assisted. There is however a difference between ethylene and propene. In ethylene, the insertions from the second onward are  $\beta$ -agostic because of the spontaneous displacement and reorientation of the chain along the substrate. Here they are  $\alpha$ -agostic at each stage,<sup>45</sup> mainly because the  $\beta$ -agostic interaction is at least partially hindered by steric interactions of the methyl group in the  $\beta$  position with the substrate, which prevents a necessary barrierless rotation from taking place.

*A priori*, a change in the chain conformation from  $\alpha$ - to  $\beta$ -agostic could be achieved by rotating the polymer chain around the torsional angle defined by  $C_\beta$ – $C_\alpha$ –Ti midpoint ( $C_2 = C_1$ ).<sup>46</sup> Because of the presence of the  $\text{MgCl}_2$  substrate, the rotation angle can range only from  $0^\circ$  to  $180^\circ$ .

These rotations were studied by performing constrained dynamics, defining constraint as the direction of the vector  $\mathbf{u} = (C_\alpha - \text{Ti}) \times (C_\beta - C_\alpha)$  orthogonal to the plane containing the metal and the  $C_\alpha$  and the  $C_\beta$  atoms. This method univocally fixes the torsion angle that represents the reaction coordinate for the switching mechanism from  $\alpha$ - to  $\beta$ -agostic interaction. The initial angle, referred to as  $0^\circ$ , is assumed to be the one with the vector  $\mathbf{u}$  orthogonal to the  $\text{MgCl}_2$  (110) surface (i.e., parallel to the  $z$ -axis of our supercell). The chosen reaction coordinate is equivalent to the one proposed by Lohrenz et al.<sup>47</sup> for a Zr-based homogeneous system. The results are shown in Figure 9, where the displacements from  $0^\circ$  to  $90^\circ$  are reported. This situation corresponds to the chain torsion required to bring the system from  $\alpha$  to  $\beta$  conformation. Rotations from  $90^\circ$  to  $180^\circ$ , in principle, need not be considered. However, we still sampled some values beyond  $90^\circ$  for the sake of completeness and found that they are energetically unfavored, due to the presence of the Cl atom bridging the Ti and the substrate. As a

(43) We observed no inversion of the *dangling* Cl atom under our simulation conditions. To this extent we can state that the site is stereorigid, in the sense that the chlorine neither occupies the free coordination site nor is interchanged with the growing polymer. The reason may be the proximity of a nearby Mg surficial site on the same layer carrying the Ti and toward which the *dangling* Cl points. This distance is in fact 3.034 Å on average (see Supporting Information) in the  $\pi$ -complex, but during the dynamics can shorten up to 2.795 Å, thus giving more stability to the site and not allowing the sterically larger polymer chain or monomer units to be interchanged with the Cl atom. Of course, we do not exclude that at later stages this Cl atom could undergo some chemical reaction through, e.g., alkylation, or that the interaction with a co-catalyst could enhance/activate inversion processes.

(44) (a) Keii, T.; Suzuki, E.; Tamura, M.; Murata, M.; Doi, Y. *Makromol. Chem.* **1982**, *183*, 2285. (b) Keii, T.; Terano, M.; Kimura, K.; Ishii, K. In *Transition Metals and Organometallics as Catalysts for Olefin Polymerization*; Kaminsky, W., Sinn, H., Eds.; Springer-Verlag: Berlin, 1988; p 3.

(45) We observed that, during the reaction, one of the two H belonging to the  $C_\alpha$ -reduced its distance from Ti to 1.897 Å with respect to its initial value of 2.639 Å. The former value refers to the transition state, and the latter to the  $\pi$ -complex.

(46) We adopt here the same notations of ref 47 on p 12 798.

(47) Lohrenz, J. C. W.; Woo, T. K.; Ziegler, T. *J. Am. Chem. Soc.* **1995**, *117*, 12 793.

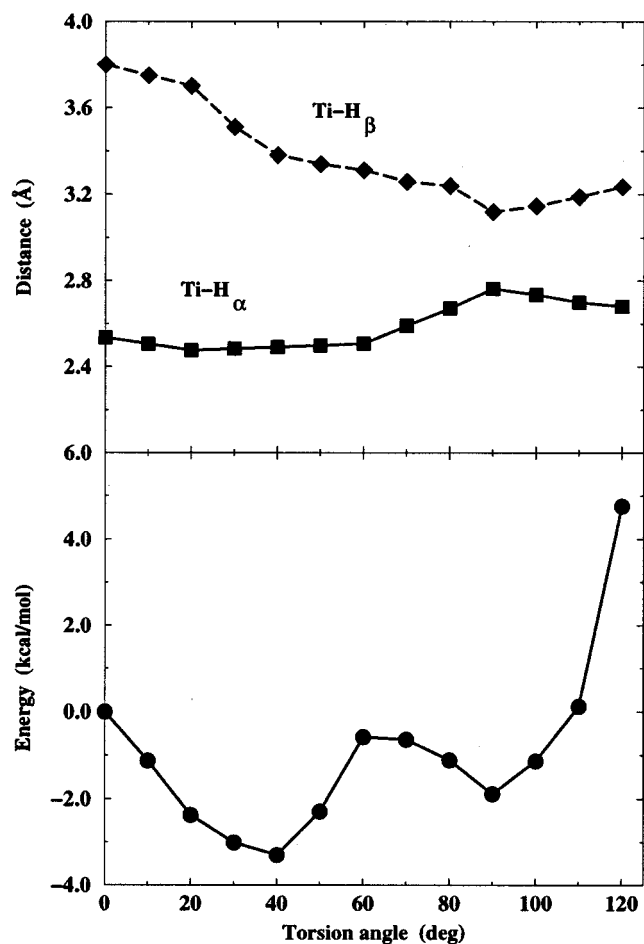


**Figure 9.** Energetics and distances of  $H_{\alpha}$  and  $H_{\beta}$  from the catalyst as a function of the reaction coordinate described in the text for the chain rotation process. Solid and dashed lines are intended only as a guide to the eye.

consequence, the  $\text{CH}_2$  group in the  $\alpha$ -position undergoes strong steric interactions approaching this Cl, which prevent the chain from completing the  $180^\circ$  rotation.

We observed that an energy decrease occurs up to  $\sim 40^\circ$ , when the chain rotation brings the  $H_{\alpha}$  far away from the substrate, thus reducing steric repulsions of the  $\alpha$ -methylene group with the Cl atoms of the support, but still keeping an  $\alpha$ -agostic interaction with the Ti atom. This conformation recovers the  $\pi$ -complex configuration already obtained with the free dynamics and is locally stable. From the  $\pi$ -complex, the system goes through a barrier of 2.7 kcal/mol to a local minimum at  $90^\circ$ . This minimum is the closest one can get to a  $\beta$ -like agostic conformation. However, because of the chain rotation and its interactions with the substrate, we are dealing here with an  $\alpha$ -like situation because  $\text{Ti}-H_{\alpha} = 2.764 \text{ \AA}$ . We have dynamically explored this minimum, performing constant-energy, constraint-free molecular dynamics for  $\sim 1.5$  ps. Indeed, we observed that the system oscillates around the  $90^\circ$  position with a maximum excursion of  $12^\circ$ , a value insufficient to overcome the barrier separating this minimum from the previous one ( $40^\circ$ ).

This result is due to the fact that the  $H_{\beta}$  is that connected to a  $\beta$ - $\text{CH}_3$  and the bulk of this residue that hinders the large displacements needed for a full switch from  $\alpha$  to  $\beta$  to take place. This lack of a switch from  $\alpha$  to  $\beta$  is clearly another important difference with respect to homogeneous catalysts.<sup>47,48</sup> These results are summarized in Figures 9 and 10.

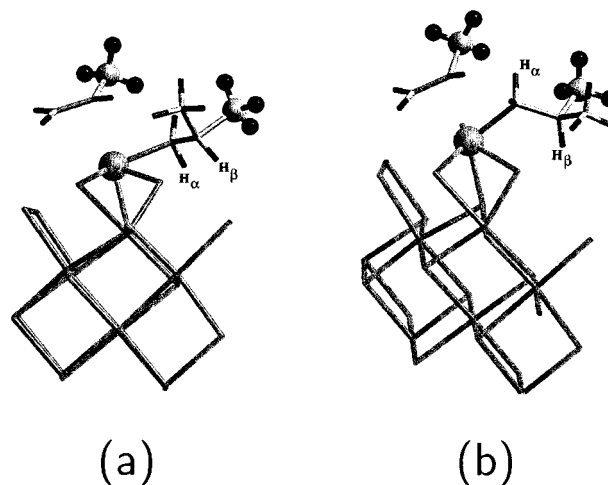


**Figure 10.** Polymer chain conformations relevant to the rotation angles of (a)  $20^\circ$  and (b)  $90^\circ$ . The rotation angles are two selected values of the reaction coordinate describing the conformation change. Details are given in the text.

We note, however, that it can be envisaged that at later stages, due to the larger flexibility of the longer chain, the agostic mechanism can take place with other H atoms (e.g., in  $\beta$  or  $\gamma$  position) in an energetically more favored or even barrierless way. This recovers one of the possible mechanisms invoked as a precursor for chain termination processes; namely, H transfer to the metal or to the monomer.

#### 4. Conclusions

We have presented a detailed study of the polymerization of propene, addressing the problem of the enantioselectivity in heterogeneous catalysis. To the best of our knowledge, this is the first time that a First Principles analysis of this kind has been attempted on a realistic heterogeneous system. We have shown that the center introduced previously<sup>13</sup> has the correct properties to produce isotactic chains. We also elucidated the mechanism involving a possible switch from an  $\alpha$ -agostic interaction to a  $\beta$ -agostic one, which can play a role in chain termination mechanisms. In this case, we have seen that the role of the support cannot be neglected because it makes significant differences with respect to sterically open systems such as the homogeneous ones.

The insertion process induces a large reorientation of the chain, which, as described, displaces along the substrate in a way very similar to the case of ethylene. This fact rules out the flip-flop aspect of the Cossee-Arlman scheme<sup>32</sup> and eliminates the syndiotactic channel<sup>49</sup> for our center. The favored orientation of the olefin approach to the active center, together with the  $\alpha$ -agostic interaction, provides support for the Brookhart-Green<sup>33</sup> picture. The remarkable fact is that the chain flips back in the way described earlier and that the flip-flop is not possible near the surface because of steric problems. This situation is significantly different from metallocenes, although possible at low propene concentrations.

The energetics resulting from our calculations relevant to propene insertions for the initiation and propagation steps are in good agreement with available experimental findings, thus providing support for the reaction pathway depicted.

(48) (a) Woo, T. K.; Margl, P. M.; Lohrenz, J. C. W.; Blöchl, P. E.; Ziegler, T. *J. Am. Chem. Soc.* **1996**, *118*, 13 021. (b) Woo, T. K.; Margl, P. M.; Ziegler, T.; Blöchl, P. E. *Organometallics* **1997**, *16*, 3454, and references therein.

(49) Corradini, P.; Guerra, G.; Pucciariello R. *Macromolecules* **1985**, *18*, 2030.

A novel application of the maximally localized Wannier functions has been used to follow the chemical reaction from the point of view of the electronic structure modifications. We have shown that even fine details, such as the agostic interaction, can be efficiently described in terms of displacements of the WFCs and their related dispersions.

**Acknowledgment.** We wish to acknowledge helpful discussions with Kiyoyuki Terakura, Pier Luigi Silvestrelli, Roger Rousseau, Paolo Carloni, and Simone Raugei as well as precious hints from Michiel Sprik for the constrained dynamics problem. We are also grateful to one of the referees for his hints and

suggestions that helped in making more clear the discussion about the WFCs technique. We acknowledge financial support from BASF AG and Targor.

**Supporting Information Available:** Equilibrium geometries of the  $\pi$ -complex, transition state and final product of the second isotactic insertion of propene. Plot of the distribution of the Ti–Cl bond lengths for the  $\pi$ -complex during the dynamics (PDF). This material is available free of charge via the Internet at <http://pubs.acs.org>.

JA990913X